Electromigration study of oxygen disorder and grain-boundary effects in $YBa_2Cu_3O_{7-\delta}$ thin films

B. H. Moeckly, D. K. Lathrop, and R. A. Buhrman
School of Applied and Engineering Physics, Cornell University, Ithaca, New York 14853-2501
(Received 18 March 1992; revised manuscript received 2 September 1992)

We report on the effects of strong electrical currents (≥ 1 MA/cm^2) applied at ~ 300 K to $YBa_2Cu_3O_{7-\delta}$ thin-film microbridges that both do, and do not contain high-angle grain boundaries. In the grain-aligned microbridges, below a certain threshold level such currents promote a slow improvement of the normal and superconductive properties of the microbridge. This behavior is attributable to the current-driven increase in basal-plane oxygen order in a manner characteristic of dispersive transport. Above threshold, the effect of the electromigration current is to create rapidly regions of strong oxygen disorder, which increases the microbridge resistance and decreases the transition temperature and critical current. This disorder shows a tendency to segregate under electromigration bias and can be at least partially removed by reversal of the current. The threshold effect permits an estimate of the atomic force required to promote the creation of oxygen disorder in $YBa_2Cu_3O_{7-\delta}$. The superconducting properties of the disordered regions have the characteristic of a composite superconductor, consisting of a network of superconducting filaments partially shunted by normal conducting paths. Comparison with the behavior of microbridges containing high-angle grain boundaries indicates that such boundaries consist of more or less random connections of these filaments.

I. INTRODUCTION

Since the discovery of the high-T_c cuprates, it has been well known that oxygen plays a dominant role in determining their structural and superconductive properties. More recently, experimental studies of oxygen-deficient $YBa_2Cu_3O_{7-\delta}$ (YBCO) single crystals[1-3] and bulk samples[4] have focused attention on the importance of understanding the oxygen *ordering* in these materials. The crucial role of this ordering in determining the carrier concentration and hence superconductive and normal-state properties is the subject of vigorous research.[5-10] There is also increasing evidence that vacancies and disorder in the basal-plane oxygen chain sites may be responsible for many of the deleterious effects of grain boundaries in these materials, an unfortunate consequence of the short coherence length as well as the high oxygen mobility ($\sim$1-eV activation energy for diffusion). Some of the effects on the properties of these grain boundaries in YBCO thin films due to the removal and replacement of oxygen have been detailed.[11] It is not yet clear, however, how this oxygen disorder affects the high-T_c superconductivity at the microscopic level or, in the case of grain boundaries, how the resulting weak-link problems can be overcome when they are unwanted or how the Josephson-like properties of such weak links can be improved when they are desired for superconductive device applications.

In this paper we report and discuss the results of an extensive series of experiments with YBCO thin-film microbridges in which the chain oxygen order has been substantially and, to a large extent, reversibly altered by the process of electromigration. The microbridges studied included those that consisted of grain-aligned material, having no high-angle tilt boundaries, as well as microbridges which contained one or two isolated high-angle (45° or 27°) tilt boundaries. The response of these microbridges to high ($\geq 1\times 10^6$ A/cm^2) current biases at ~ 300 K was quite unusual, with a clear threshold being found for the onset of destructive effects due to the creation of oxygen disorder. Below this threshold the effect of an applied current is to slowly improve the normal-state and superconductive properties of the microbridge. From these measurements and studies of the properties of the microbridges subsequent to the imposition of controlled electromigration biases, some insight has been gained into the superconductive character of YBCO thin films that contain regions of strong chain oxygen disorder. Comparison of the behavior of disordered material with and without grain boundaries has led to a phenomenological model that helps explain the strongly detrimental effect of grain boundaries in nonideal (i.e., locally oxygen deficient) YBCO.

Although to our knowledge this work represents the first controlled and reversible study of oxygen electromigration in YBCO thin-film microbridges with and without grain boundaries, there are a few related studies in the literature. Vitta *et al.* studied the electromigration-induced failure of YBCO thin films involving the movement of cations.[12] Rajan *et al.* observed the electromigration of oxygen in bulk sintered rods of YBCO at very low current densities and elevated temperatures.[13] Large reductions in the critical currents of YBCO thin-film lines by high current pulsing have been seen by Robbes *et al.*, although the cause of this effect was not clear.[14] And a study of Ag-YBCO point contacts by Rybal'chenko *et al.* reports a reversible switching of the current-voltage characteristics to different levels of excess current when a high voltage bias is reached.[15]

II. THIN-FILM PREPARATION AND PROPERTIES

A. General characteristics

Our films, which are ~300 nm thick, were deposited onto single-crystal (001) MgO substrates using the ubiquitous method of pulsed laser ablation. Deposition was performed at 248 nm and 50 Hz using a laser fluence of ~1 J/cm^2. The substrates were heated to 670 °C in a 400-mTorr oxygen ambient. Targets were either made by us or obtained from Jupiter Technologies, Inc. The films are completely *c*-axis oriented, and we control the in-plane epitaxy of the YBCO by properly preparing the surface of the substrate.[16] That is, we are able to obtain films with either no high-angle tilt boundaries or with a fraction (10–20 %) of 45° or, in some cases, 27° tilt boundaries. The films were patterned using inert-ion etching to form microbridges 1–2 μm wide and 2–6 μm long. In this way, we are able to study the properties of both "grain-aligned" microbridges (those containing no high-angle tilt boundaries and having J_c's as high as 5 MA/cm^2 at 77 K) and microbridges containing high-angle tilt boundaries and displaying Josephson weak-link behavior.[16,17]

An example of the resistive transition and *I-V* characteristic of a microbridge patterned in a film that does not contain high-angle tilt boundaries is shown in Fig. 1. As is typical for films grown on MgO, the transition, while reasonably abrupt, is suppressed a few degrees (~2–4 K) below values usually obtained for both the bulk material and grain-aligned films deposited on lattice-matched substrates. This behavior is generally attributed to the presence of strain and defects in the film that result from the ~9% lattice mismatch for *c*-axis normal YBCO films on MgO. The resistivities ρ_n of our best grain-aligned films (~60 $\mu\Omega$ cm at 100 K) are comparable to the best results obtained with carefully annealed twinned crystals.[18–20] These films have the nearly linear temperature dependence of single-crystal YBCO ($\rho_n \approx aT$), although extrapolation to zero temperature sometimes yields a negative resistance intercept. This result has occasionally been attributed to the existence of a $YBa_2Cu_4O_{8-\delta}$ phase, although no detectable amount is seen in the x-ray analysis of our films, and, perhaps more significantly, the negative intercept is also seen in single crystals of YBCO.[18–20]

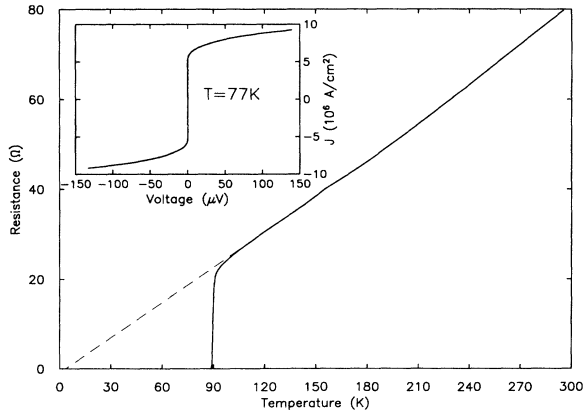

FIG. 1. The resistive transition and *I-V* characteristic at 77 K for a microbridge without high-angle tilt boundaries. The J_c at 4.2 K was 5.5×10^7 A/cm^2.

Films containing high-angle tile boundaries, on the other hand, often display a positive zero-temperature resistance intercept, and the resistivities of these films are typically two to three times higher than grain-aligned films. The zero-temperature resistance offset of these films is likely due to the temperature-independent resistance of high-angle grain boundaries, but the increased temperature-dependent resistivity must be accounted for by an increased defect density in the grains themselves. Rutherford backscattering spectroscopy (RBS) utilizing high-energy oxygen resonance scattering[21] clearly shows, in fact, that the χ_{min} values for ion channeling (*including* oxygen) are increased significantly in films containing high-angle tilt boundaries.[16] RBS analysis also confirms that even the best films are not fully oxygenated ($\delta=0$).[22] In general we have found that extended oxygen annealing efforts fail to improve this situation. Despite, or perhaps because of, this oxygen deficiency, those films which do not contain high-angle tilt boundaries exhibit very high critical current densities in both zero and in high magnetic fields (see Fig. 1). These J_c values are quite similar to those typically reported for quasi-single-crystal thin films grown on $LaAlO_3$ and $SrTiO_3$.[23]

B. Transport properties and oxygen-defect distribution

Following the laser-ablation deposition process our films are slowly cooled to nearly room temperature in pure oxygen to allow any oxygen disorder in the film to have sufficient time to equilibrate with the local thin-film environment. This equilibration is demonstrated by the fact that the film properties are stable over extended times at ~300 K and under limited excursions to higher temperatures, ~400 K. The significance of the equilibration process is emphasized by the observation that these "slow-cooled" films have a distinctly different temperature-dependent resistance behavior from that obtained by rapid thermal annealing the films in an oxygen environment for a minute or two at a moderate temperature (750 K) and then "quenching" to room temperature (a cooling time of ~2 min). A similar effect may be obtained by a rapid thermal argon anneal for a few seconds followed by a short rapid thermal oxygen anneal.

After such a quench, the effect of which can be reversed by a subsequent anneal and slow cool, the resistance of the film increases by ~50% or more and the *R* vs *T* curve invariably takes on a "bowed" shape as illustrated in Fig. 2. This characteristic shape can be seen in the thin-film data of several authors, yet its origin is never discussed. We have observed that such curves can be well fit by a phenomenological model consisting of *two parallel conduction paths*, one of which has a resistance characteristic of clean, fully oxygenated $YBa_2Cu_3O_7$ in the normal state, while the other has a temperature-independent resistance. This implies that the quenching process creates inclusions of disordered material within the film. These regions reduce the amount of material

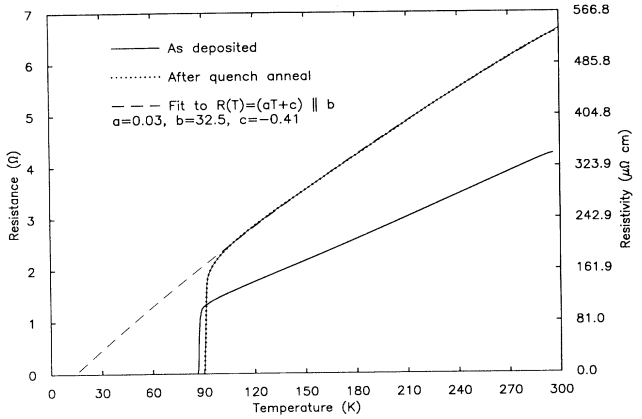

FIG. 2. The resistive transition for a film that has been thermally "quenched" from 450 °C after a 10-s argon anneal followed by a 10-s oxygen anneal. The shape of the curve can be fit by a model consisting of two parallel conduction paths, i.e., $R_n=(aT+c)\|b$, indicating the existence of small inclusions of disordered material within the film.

which has the characteristic normal-state resistance of $YBa_2Cu_3O_7$ and provide an additional parallel contribution to the overall film resistance that is at least approximately T independent, with a magnitude that depends on the degree of disorder.

In addition to the increase in the magnitude and the change in character of the normal-state resistance, the superconductive critical current of a "grain-aligned" microbridge following a quench anneal is also significantly reduced, typically by about a factor of 3. A direct transport measurement of the critical current I_c of a microbridge measures, of course, the weakest section of the microbridge, while the resistance is a better, but far from perfect, measure of the average behavior of the entire microbridge. Keeping that distinction in mind, we find that if the decrease in I_c is attributed to a reduction in the original volume fraction of superconductive material, the change is roughly consistent with the increase in the linear temperature-dependent term in the resistance of the quenched film which would result from a loss of superconductive material.

The results of these simple experiments offer initial insight into the importance of the distribution of oxygen defects within the films. It is known that when YBCO is cooled from the high-temperature tetragonal phase to the low-temperature orthorhombic phase, the oxygen ions that formally provided a 50% occupancy of the interchain O(5) lattice sites move to previously vacant O(1) chain sites, forming, in the ideal case of $\delta=0$, the fully occupied oxygen chains in the b-axis direction. (Our lattice site notation follows that of Ref. 24.) This oxygen configuration is the Ortho-I phase.[7] These ordered oxygen chains provide carriers to the conduction planes via proper coordination of the basal-plane Cu(1) atoms.[5–10] This mechanism for hole doping seems to be well established. Recent studies[1–4] of rapidly quenched bulk and single-crystal YBCO have shown that in the case of oxygen-deficient material the degree of chain-site ordering that is present can strongly affect the superconductive properties (T_c) of the material. To explain this result Veal and Paulikas[10] argue that placing an oxygen ion on a vacant site that links two disconnected Cu-O-Cu chain elements adds two holes to the adjacent conduction planes, while extending an existing Cu-O-Cu chain by one unit adds one hole, and creating an isolated Cu-O-Cu unit adds none. Thus, local rearrangements of the same average density of oxygen chain vacancies can have a striking impact on the local transport properties of the material. The annealing studies of quenched oxygen-deficient YBCO show that the equilibrium state tends to be that which maximizes chain order (chain length) and the average hole concentration. Unfortunately, it appears that the energy cost for disrupting this order is quite low.

Jorgensen *et al.*[24] suggest that an effect of a chain vacancy is to disrupt the structural coherence of the CuO_2 conduction planes which could destroy superconductivity locally in the same manner as other structural defects in the CuO_2 plane. If so, a small aggregation of such vacancies in parallel in a given YBCO basal plane should produce a region through which the transport in the CuO_2 conduction plane is severely weakened. A possible consequence is that transport can proceed only by inelastic tunneling or by "detour" transport in the c-axis direction to adjacent CuO_2 planes which are bounded by properly occupied chain sites. Friedmann *et al.*[25] have found that the c-axis resistivity of very carefully annealed YBCO is metallic but not strongly temperature dependent. In either case the effective resistance of a sufficiently small region of locally disordered material can be expected to be at least roughly T independent, in accord with our result. To investigate further the effect of the oxygen-defect distribution and to probe these effects on a more local scale, we undertook the following electromigration experiments.

III. ELECTROMIGRATION OF GRAIN-ALIGNED MICROBRIDGES

The electromigration experiments described here consisted of examining the consequences of the application to the microbridges of a high, constant dc current bias ($1-7$ MA/cm^2) at room temperature in a helium ambient. We have studied both quenched and slow-cooled microbridges. The temperature of the microbridges was, of course, raised due to self-heating. The actual microbridge temperature during electromigration was deduced by extrapolation of the temperature-dependent resistance of the microbridge at the beginning and end of application of the current, essentially using the YBCO microbridge as a thermometer. In general, changes in the microbridge resistance due to electromigration effects occurred over a time scale very long compared to the thermal equilibration that follows the initial application of the current, so a reasonably accurate estimate of sample temperature during the electromigration process could be made. The device resistance was monitored during the application of electromigration bias, which typically was applied for up to 24 h, and transport measure-

ments were subsequently used to characterize the normal-state and superconductive properties of the films.

A. Healing

We will first discuss the behavior of grain-aligned, slow-cooled microbridges. The bridges studied had initial J_c's of 2×10^6–6×10^6 A/cm^2 at 77 K. The first effect observed as a result of a high current bias in these films was a slow "healing" or improvement of both the normal-state and superconductive properties which took place gradually over a period of many hours. This process occurs for a bias current density (J_{EM}) of 3–5 MA/cm^2 which typically results in self-heating of the microbridge to a temperature in the range 330–370 K. As a result of this process the normal-state resistance (R_n) of the microbridge is decreased by as much as 5–10%, and J_c is increased by typically 10–20%. Sometimes a slight increase in T_c is observed, but no change or even a slight decrease is perhaps just as likely. An example of this healing behavior and its consequences is shown in Fig. 3.

It might be thought that this behavior is the result of a simple heating effect, since the temperature of the microbridge is indeed raised by ~50 K upon application of the current densities used. While heating certainly increases thermally activated defect motion, this explanation alone is insufficient to account for all the observed effects. To examine this question, we have measured the resistance vs time and the transport properties for several microbridges that were simply heated to 335–390 K in vacuum or in an oxygen ambient. The normal-state resistance of the bridges after these anneals usually remained the same, although sometimes a slight rise was seen (~2%), with the time dependence during heating being more or less linear. We have observed *no* decrease in R by heating alone, nor have we observed a time dependence of R during heating at all similar to the time dependence (discussed below) of the current-induced healing effect.

We conclude that the healing effect, which will occur for either direction of applied bias, is a consequence of the bias current driving a beneficial redistribution of chain oxygen vacancies within the microbridge. This hypothesis is, of course, consistent with the slight oxygen deficiency of our films, so that oxygen vacancies certainly exist, allowing changes to be effected in the oxygen ordering. The result may either be an overall increase in the degree to which the O(1) oxygens are ordered into the extended chains of the ideal Ortho-I phase of YBCO, increasing the overall carrier concentration, or simply the development of a more uniform distribution of the vacancies throughout the microbridge so as to reduce their impact on the transport properties, or a combination of these two processes.

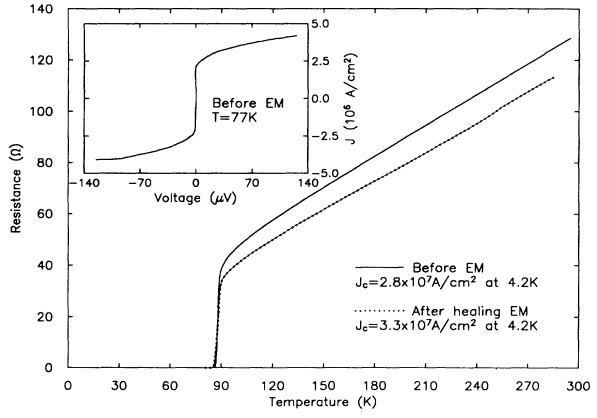

FIG. 3. The resistive transition for a grain-aligned microbridge that has been improved by application of a current bias of 5 MA/cm^2 for over 6 h. R_n has been decreased by 10% and J_c has been increased by 15%.

In the standard semiclassical model of electromigration, the effect of an applied bias is to influence the net displacement of mobile atomic species in a direction either parallel or antiparallel to the direction of the applied current, depending on the effective valence of the mobile ion. The driving force is a combination of the effects of the "electron wind" and the applied electric field in altering the local atomic potential for thermally activated diffusion. Experiment has indicated that the direction of chain oxygen anion movement in YBCO in response to an applied bias is towards the cathode,[13] indicating that the momentum transfer from the hole wind dominates the electromigration force in this system. But in typical electromigration experiments even at current levels as high as 10^7 A/cm^2, the changes in the activation energy for diffusion in the preferential direction are $\ll kT$. Thus, as in any activated diffusion process in the presence of a weak driving force, only ions that have sufficiently low activation energies that they can fluctuate rapidly on the experimental time scale will respond to the electromigration bias.

Experimental measurement of oxygen tracer diffusion in the *a-b* plane of single-crystal YBCO yields a value of 0.97 ± 0.03 eV for the activation energy;[26] independent measurements of oxygen ordering in quenched crystals appear to confirm this value.[2] The resulting in-plane oxygen diffusion constant has been measured to be $D_{ab}=1.4\times10^{-4}\exp(-0.97\ \text{eV/kT})\text{cm}^2/\text{s}$.[26] Therefore, the oxygen mobility is expected to be relatively low at 300–350 K, and application of the electromigration force should only result in net displacements of the chain oxygen ions over near-atomic distances, ≤ 1 nm, during the time scale of the experiment. However, recent measurements have indicated that the diffusion constant D_b for oxygen motion in the *b* direction is at least 100 times greater than the diffusion constant in the *a* direction D_a.[27] A possible explanation for this result is found in the calculation of Ronay and Nordlander,[28] who find a zero-value activation energy for movement parallel to the *b* axis in the region between the CuO chains [along the normally unoccupied O(5) sites]. It has been suggested[27] that oxygen diffusion in the *b* direction occurs by a process whereby an oxygen ion at the end of a string of occupied O(1) sites jumps to an adjacent, normally unoccupied O(5) site and then moves along the O(5) sites until it is adjacent to another unoccupied O(1) site, which it occupies. If the activation energy for the O(1) to O(5) displacement is ~1.0 eV while the activation energy for ox-

ygen diffusion from O(5) to O(5) sites is indeed considerably lower, then the O(1) to O(5) jump is the rate-limiting step. Thus, there may be a longer-range displacement of oxygen ions during room-temperature annealing and in the present electromigration experiments than that which the measured activation energy for oxygen diffusion would otherwise suggest.

As shown in Fig. 4, the time dependence of our current-induced healing process invariably follows a "stretched-exponential" functional form,

$$R(t)=R(\infty)-[R(\infty)-R(0)]\exp[-(t/\tau)^n], \quad (1)$$

where we find that $n=\frac{1}{2}$ can generally fit the data, but that other values of n, 0.3–0.7, often provide better fits. This stretched-exponential or Kohlrausch behavior is a general characteristic of relaxation in complex systems.[29–31] It is perhaps most simply attributable to the thermally activated relaxation of an array of elements which have a distribution of activation energies. The behavior is often taken to be indicative of an overall relaxation process which is governed by dispersive transport of defects[32] or by strong interactions between elements of the relaxing system.

A closer examination of the time-dependent resistance often reveals small transient departures from the functional form of Eq. (1), suggesting that series kinetics are indeed involved in this time-dependent current-induced process. In Fig. 5 we show the relaxation in R that was seen during two consecutive current biases, the first at 3.8 MA/cm^2 and the following one at 5 MA/cm^2. The nature of this transient behavior is evident principally as a fairly sudden onset of an increasing R followed by a less abrupt return to a decreasing R at a rate that gradually approaches that predicted by the overall stretched exponential fit. As can be seen in the figure, this behavior was remarkably reproducible from the first to second run, although the time scale for the occurrence of the transients is lengthened in the case of the second, higher bias measurement. It appears that the resistance relaxation process is indeed quite complex, with an initial reduction in R (decrease in net oxygen disorder) opening a conduit whereby the driving force results in a brief increase in R (increase in net oxygen disorder) which is then followed by a further reduction in R (additional decrease in oxygen disorder).

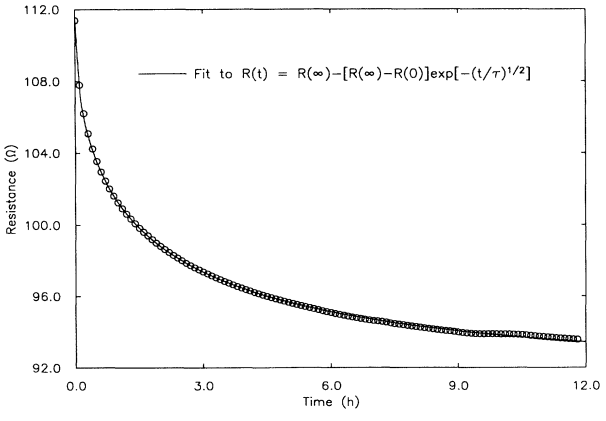

FIG. 4. The resistance of a grain-aligned microbridge vs time during a healing electromigration. The time dependence of this current-induced healing process is well fit by a stretched-exponential functional form [Eq. (1)]. The current bias in this case was 3.5 MA/cm^2.

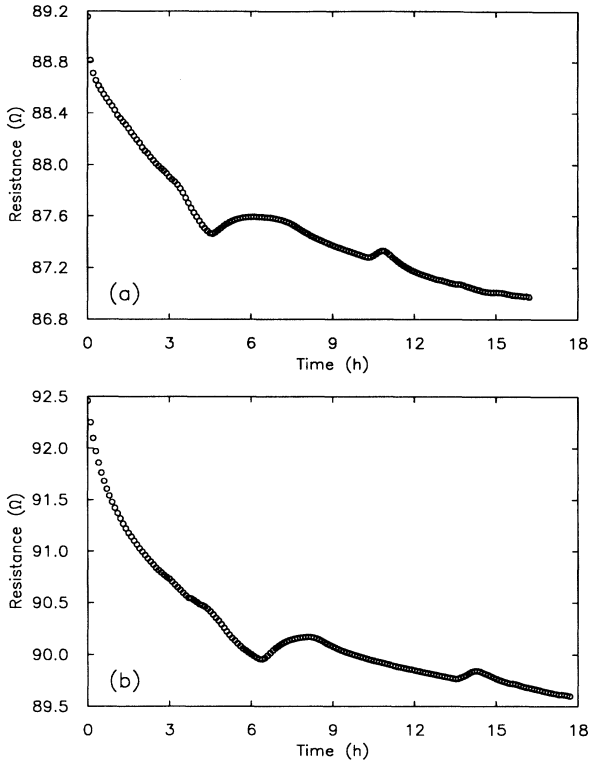

FIG. 5. The time-dependent resistance during an electromigration process often reveals small transient departures from a strict functional form. Both curves are taken from the same device for two current biases. The bias was applied in the same direction in both cases and had a magnitude of 3.8 MA/cm^2 in (a) and 5 MA/cm^2 in (b).

Jorgensen *et al.*[4] and Veal *et al.*[2] have found that the same stretched-exponential function (with $n=\frac{1}{2}$) can describe the time dependence of the rise in T_c of quenched, oxygen-deficient bulk polycrystalline and single-crystal YBCO upon room-temperature annealing. This indicates that this time dependence is a general consequence of the complex nature of the local ordering process in YBCO and is not necessarily a result of the thin-film form of the material being studied here.

Other functional forms,

$$R(t)=R(\infty)-[R(\infty)-R(0)][\tau/(t+\tau)] \quad (2)$$

and

$$R(t)-R(\infty)\sim t^{-m}, \quad (3)$$

have also been proposed to describe the increase in T_c of quenched YBCO single-crystal and ceramic samples. Equation (2) is an empirical relation that has been successful in describing the dynamics of some phase transi-

tions, while Eq. (3) (with $m = \frac{1}{2}$) is derived from a scaling dynamics model calculation of oxygen ordering in the *a-b* plane of YBCO.[33] While the data of Jorgensen *et al.*[4] and Veal *et al.*[1,2] are not sufficient to determine whether Eq. (1), (2), or (3) provides the best description of their results, in our case neither of the latter two functions provides a good description of the current-induced relaxation of the microbridge resistance. Of course, the agreement with one of the time-dependent models proposed by Jorgensen may be fortuitous. And while healing does appear to be attributable to a redistribution of oxygen vacancies, it is not clear how the presence of a driving force should affect any model that is concerned with the growth of ordered domains.

B. Degradation

At only slightly higher current densities ($J_{EM} \sim 5-7$ MA/cm^2) the effect of electromigration is invariably to degrade rapidly the electrical properties of the microbridge. The severity of the change is determined by the magnitude of J_{EM} and by the amount of time the current is applied. R_n of the microbridges is almost always increased in this process. In limited duration (~ 60 s) electromigrations at a bias just above ($\leq 20\%$) the threshold, we have obtained increases in R_n of up to 80%; with an extended bias period of several minutes R_n has been increased by about a factor of 3. The critical current density is typically reduced by an order of magnitude by such destructive electromigrations. As we show below, this degradation, if limited, is at least partially reversible by subsequent electromigrations at lower biases and opposite sign. A larger J_{EM} (≥ 7 MA/cm^2) or a more extended period of destructive electromigration may cause J_c to be reduced by more than a factor of 10^4. In addition, T_c may be reduced to just a few degrees or the sample may be made insulating or semiconducting. An illustration of this behavior is given in Fig. 6. However, following such a result the original properties of the microbridge can be completely recovered by a brief oxygen anneal at 450 °C.

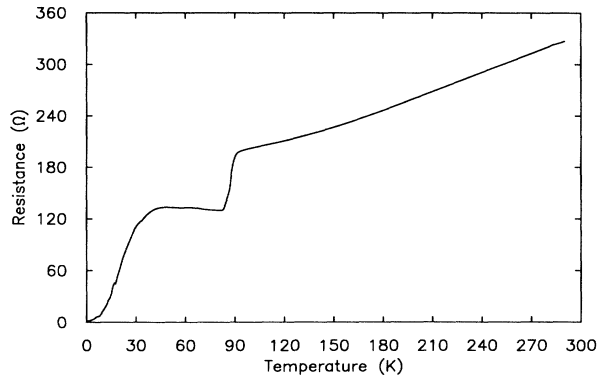

FIG. 6. High current biases can cause significant oxygen disorder in the YBCO microbridge; T_c may be reduced to very low temperatures or the sample may display semiconducting or insulating behavior. This curve was the result of an electromigration bias of ~ 7 MA/cm^2. Note the high normal-state resistance; the bulk transition, however, remains clearly defined.

The usual outcome of a destructive electromigration of limited duration is the creation of one or more localized regions of disorder within the microbridge. This is indicated by the fact that a limited duration electromigration typically results in an R vs T curve that extrapolates to a positive resistance intercept at $T=0$, where previously there was a zero intercept. This is illustrated in Fig. 7(a). A slightly stronger, or more extended, electromigration bias often results in the appearance of a "foot" in the resistive transition as shown in Fig. 7(b). The resistance of the microbridge between the bulk of the transition and the foot is roughly temperature independent and if the foot resistance is subtracted, the normal-state R vs T data would extrapolate fairly closely to $R=0$ at $T=0$. Both of these phenomena (positive residual resistivities and feet) are regularly seen in samples containing high-angle tilt boundaries and generally are indicative of the presence of one or more "weak links" in the sample. (See Sec. IV A.) Other evidence indicating the formation of weak-

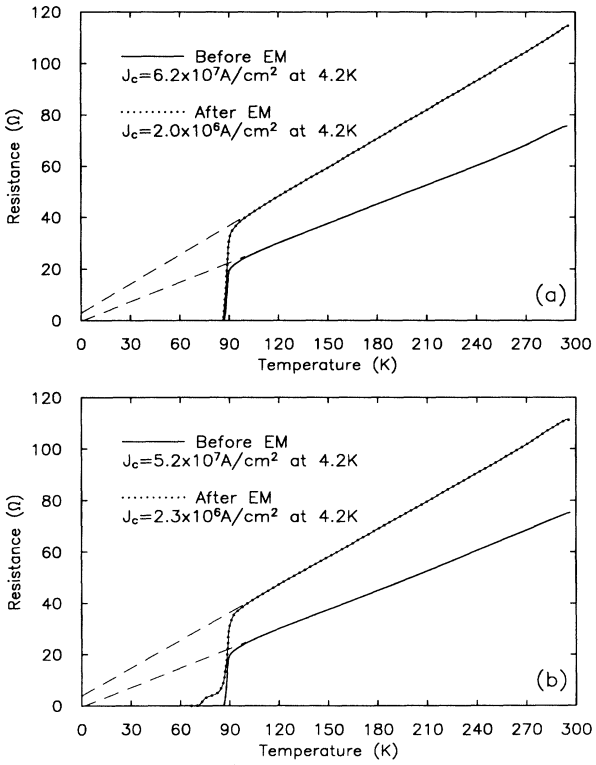

FIG. 7. Resistive transitions before and after destructive electromigration processes. In (a), a bias of 6 MA/cm^2 was applied to the microbridge for 30 s. R_n was increased substantially, J_c was reduced by more than an order of magnitude, and a positive residual resistivity was created, indicating the existence of an area of disordered material. The transition in (b) was obtained from a different microbridge by applying a bias of 6 MA/cm^2 for a few seconds. Similar behavior to that in (a) is seen. In addition, a "foot" is created in the transition, indicating the formation of a localized region of weakened superconductivity.

ened regions is obtained from the magnetic field data and the functional form of the change in resistance with time during subsequent electromigrations, which will be discussed below. An important point is that the degree of the degradation must be relatively uniform across the length of the disordered region of the microbridge, otherwise the final transition to zero R would be spread out over a wide temperature range.

Figure 8 further illustrates this creation of "uniformly disordered" regions by the destructive electromigration. The data are from a microbridge which initially had a high J_c and a flux-creep I-V characteristic. The figure shows the behavior after a series of electromigrations. J_c has been reduced by 3 orders of magnitude and a large foot in the resistive transition has developed. Notice the shape of the I-V curve: the onset of dissipation is reasonably sharp and continues quickly to an ohmic line whose resistance is close to that displayed by the microbridge in the temperature region between the bulk of the transition and that of the foot. This I-V characteristic is reminiscent of the behavior predicted by the resistively shunted junction (RSJ) model and indicates the existence of a somewhat localized region of weakened, but uniform, superconductivity. The response of this microbridge to microwave radiation, however, was quite poor; Shapiro steps were not readily observed. Thus, the region of disorder, while localized, is still largely *extended* on the scale of the superconductive coherence length.

Since the electromigration biases are sufficient to significantly self-heat the microbridge, it is important to establish that the observed degradation is due predominantly to the electromigration force and not to the ohmic heating. Simply heating unmigrated samples to 100 °C had no significant effect on their properties, as discussed previously. We have also not observed damage to a localized region, reductions in J_c, or large increases in R_n by simple heating. These effects, as described above, occur only with the presence of a high current.

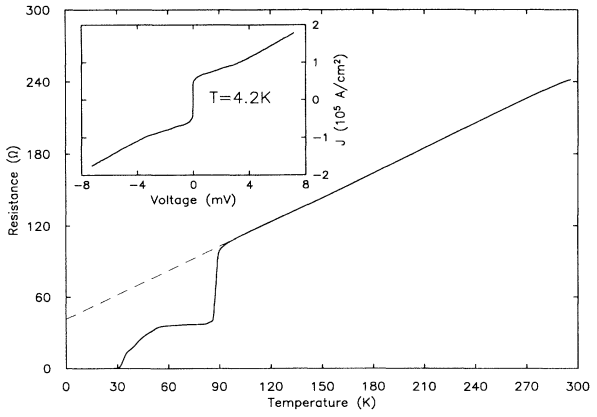

FIG. 8. The behavior after several electromigrations of a grain-aligned microbridge which originally had a J_c of 3×10^7 A/cm^2 at 4.2 K. The shape of the resulting I-V characteristic is reminiscent of RSJ behavior.

C. Reversibility

One of the remarkable aspects of this destructive electromigration behavior is that the effects are to a large degree reversible. This is achieved by reversing the direction of current flow. In fact, a change of current direction is required to reverse the effects of electromigration damage. If we have a microbridge that has been degraded by a large J_{EM} as, for example, in Fig. 7, the application of a lesser current in the same direction as the original current has no effect. If, however, the current is reversed and has a magnitude in the 3–5 MA/cm^2 range, the microbridge is healed in much the same way as discussed above: the normal-state resistance is decreased to nearly its original value, J_c is increased close to the original value, and the foot in the transition disappears. An example of the effect is shown in Fig. 9, which illustrates the reversal of the damage done to the microbridge of Fig. 7(b).

After reversal of electromigration-induced damage, an increase in the current will again cause degradation effects as before, which can be reversed by changing the current direction. J_c and $1/R_n$ can be raised and lowered in this manner, and the foot in the resistance transition can be raised or lowered, at will, by 20 K or more. The reversibility remains after several cycles of current direction. It is difficult, however, to return to 100% of the original properties after severe damage has been done. Also, after a severe electromigration or several cyclings, the restorative effects are less dramatic.

The effects associated with the *direction* of current flow strongly demonstrate the necessity of a directed particle flux. A change in the temperature gradient over a region on the order of a micron due to a simple change in direction of the current is unlikely. To test the effect of heating, samples that had been degraded were also heated to 350–390 K without applying a bias. Heating in these microbridges was found to cause an increase in J_c and an increase in T_c of the weakened region. The foot on the transition could be reduced and a rise in J_c could be continued by subsequently higher-temperature anneals. Al-

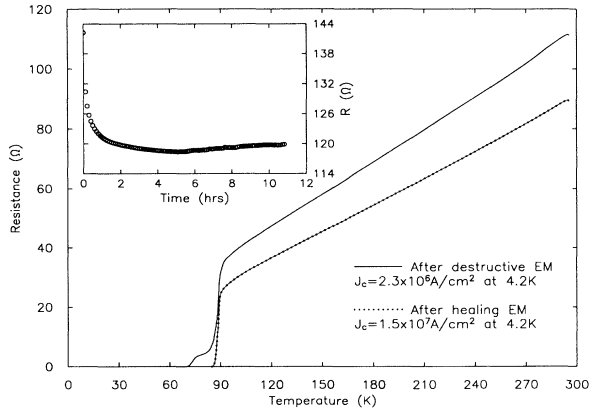

FIG. 9. This figure shows the reversal of the damage done to the microbridge shown in Fig. 7(b) by applying a current bias of 5 MA/cm^2 for 11 h in a direction opposite to the previous bias.

though weakened or damaged regions of the microbridge could be improved, decreases in R_n and restoration to a previous J_c could not be accomplished by heating alone. Again, a large bias is required to produce these effects.

We have also observed small changes of the properties of damaged microbridges with extended storage (several months) at room temperature. Initial observations indicate that J_c and R_n both increase very slowly over time for microbridges that had been degraded by electromigration. This behavior is very similar to the effect of heating. These latter observations indicate that the regions of oxygen disorder created by electromigration are slowly reordering with time and/or temperature. Increases in T_c of the disordered region with time during extended storage at 300 K have not been observed, however.

D. Quenched films

The transport properties of microbridges fabricated in films that have been thermally quenched are not improved by the application of an electromigration current at a level which usually promotes healing. Rather, the properties are rapidly degraded as illustrated in Fig. 10; R_n is increased, a foot develops in the transition, and J_c is reduced. There is some indication in the R vs T data, however, that the transport properties of the bulk of the microbridge are actually being improved: the curvature in the temperature dependence above T_c is diminished, and if the contribution of the foot to the overall resistance is subtracted, the microbridge resistance is actually less than before. This indicates that the electromigration force is segregating the disorder created by the quench into separate regions of higher and lower defect density.

E. Magnetic field results

The dependence of the critical current of the microbridge on magnetic field H as determined from the I-V characteristic was measured repeatedly between electromigrations at high bias for several of our microbridges. We note again that this type of measurement determines the critical current of the weakest cross-sectional region of the microbridge. The field was applied parallel to the YBCO c axis. Figure 11 presents J_c data measured at 4.2 K for one such microbridge where J_c is the average value as determined by the measured critical current and cross-sectional area of the microbridge. The data shown encompass electromigration-induced variations in J_c of 3 orders of magnitude and zero resistance T_c's between 31 and 90 K. The differences, which are not particularly pronounced, in the scaled J_c behavior at low H are attributed to spatial inhomogeneities across the weakest cross section of the microbridge, i.e., that part of the microbridge which is responsible for the foot in the transition. If this cross section contains spatial variations in J_c (arising from oxygen disorder) which have an average correlation length ξ, the result, due to the limited size of the sample, would be variations in the suppression of the critical current by H until the mean fluxoid spacing is $\leq \xi$. The scaled J_c vs H curves converge at about $H = 0.5$ T, which is typical of all the microbridges examined in this study, yielding $\xi \leq 60$ nm.

For $H \geq 0.5$ T the functional dependence of J_c on H is

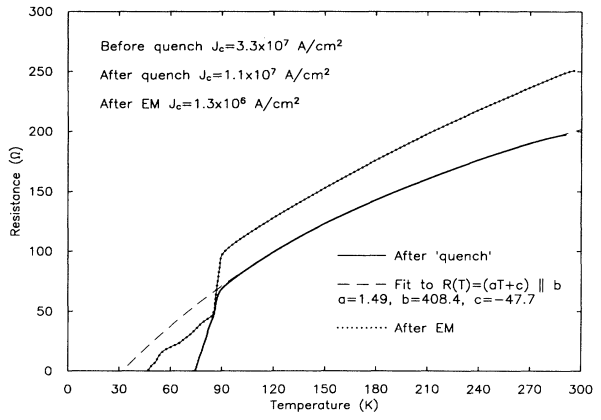

FIG. 10. Shown here is the behavior after a quench anneal at 450 °C for 60 s of the microbridge shown in Fig. 3. The properties are degraded somewhat by the quench, and these properties are further degraded by application of a current bias of 5 MA/cm^2, the same bias level that originally improved the properties of the microbridge.

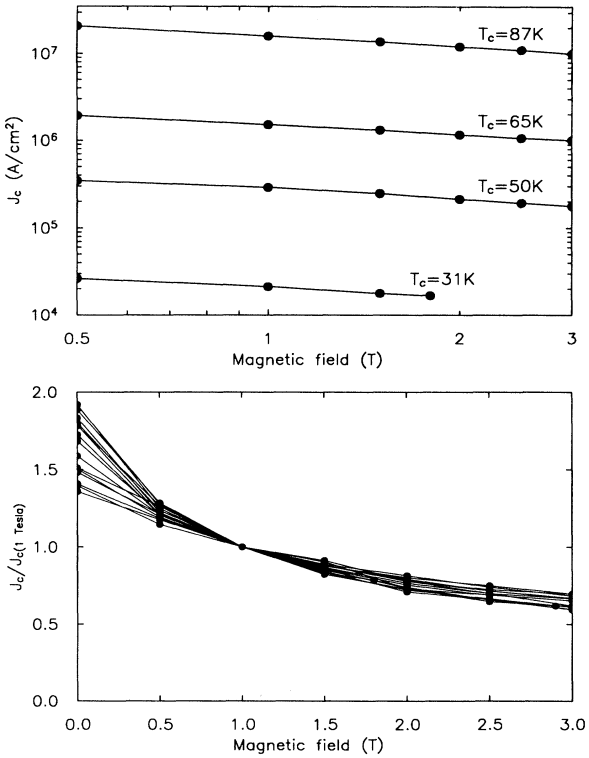

FIG. 11. The magnetic field behavior was studied for a single microbridge as a function of changes brought about by electromigration. 16 data sets are shown here. The dependence of J_c on H is nearly invariant over a very wide range of I_c (75 μA to 65 mA) and T_c (31–90 K) values.

nearly *invariant* despite the wide variation in the magnitude of J_c and the significant variation in T_c. The differences in the low- and high-field behaviors suggest that the high-field result is indicative of the "intrinsic" properties of the weakened region. Thus, the redistribution, or disordering, of the chain oxygen and the major changes in T_c brought about by the electromigration does not represent a pronounced change in the local pinning strength or indicate a major change in other *local* superconductive properties. Instead, as we discuss below, the magnetic field data indicate that the dominant effect of electromigration is to produce a wide variation ($> 10^4$) in the amount of superconductive material effectively present in the disordered region of the film.

F. A model of the superconductive character of disordered regions

In Fig. 12 we show the variation in J_c with T_c, as determined by the microbridge zero resistance, that was obtained with one microbridge during the course of an extensive series of electromigration-induced changes. The data, which include cases where J_c and T_c were both increased and decreased by electromigration currents, show a rather remarkable exponential variation of J_c with the transition temperature of the disordered region of the microbridge. Similar results were obtained with other electromigrated microbridges. This is a much stronger variation than would be expected to result from a simple reduction in T_c due to a change in carrier density with increasing chain disorder. If, for example, J_c was determined by the ideal depairing limit,[34] reductions in T_c should only suppress the low temperature J_c more or less linearly. Alternatively, formation of local regions of material well ordered into the Ortho-II phase should not so strongly depress J_c.

The experimental evidence indicates that the disordered material is a composite system consisting of a network of superconductive filaments imbedded in a nonsuperconductive matrix. As the degree of oxygen disorder increases, the fractional cross-sectional area of the material that is bridged by continuous superconductive filaments drops rapidly. The decrease in the effective T_c of the filaments does not appear to be the major factor in the decrease of J_c but simply a less strong indicator of the overall increase in oxygen disorder. The rapid decrease in J_c is instead a consequence of the tendency for chain vacancies to locally segregate, which, with increasing disorder, rapidly diminishes the probability of maintaining continuous superconductive paths through the material. As determined from the magnetic field dependence of J_c, the average lateral dimension d of these individual filaments is somewhere in the range $\xi_{ab} \leq d \leq \zeta$, where ξ_{ab} is the superconductive coherence length.

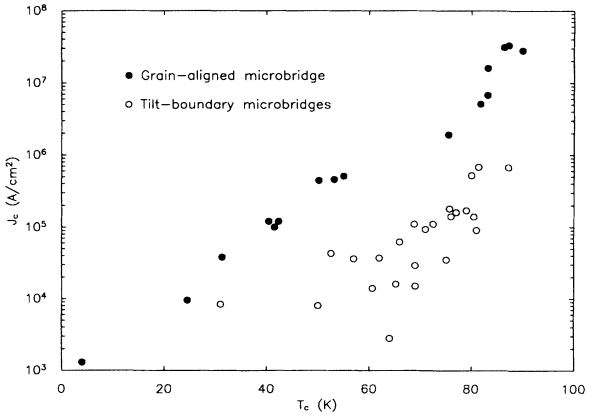

FIG. 12. The solid circles show the critical current density at 4.2 K vs zero-resistance T_c (the T_c of the "foot") for a *single* uniform microbridge that was migrated several times. The open circles show similar data for several different (unmigrated) tilt-boundary weak links.

This filamentary model can account for the resistive behavior of the highly disordered material. If, as the quenched film data suggests, in small localized regions where oxygen disorder has disrupted the normal transport in the a-b plane, the conductivity is determined by in-plane incoherent tunneling or by c-axis transport, then as more and more of the superconductive connections are disrupted this conductivity will begin to dominate, resulting in the T independent resistance of a strongly disordered region. As this disorder increases, this shunting conductance that bridges superconductive filaments becomes less effective as the average separation between these filaments grows. Thus, the temperature-independent resistance increases until eventually, when all but a very few superconductive connections are broken, the conductivity of the composite system begins to be dominated by hopping transport.

G. Discussion of the response to electromigration bias

Perhaps the most striking feature of the electromigration experiments is the sudden change with increasing bias current from slow improvement to rapid degradation. The degradation appears to be clearly attributable to the disordering of the chain oxygen by the electromigration force. The somewhat higher temperature (~ 380 K) to which the microbridge is self-heated by the increased bias level can partially account for the much faster rate of change of the electromigration effect, but the change in character from healing to degradation can only be explained in terms of the electromigration force reaching some critical threshold. We tentatively conclude that below this threshold the net rearrangement of the basal-plane oxygen is dominated by the free-energy gain associated with increased Ortho-I order. The electromigration force appears to effectively give the less-ordered (less strongly bound) O(5) ions a drift mobility so that the increased order can be attained. But above the degradation threshold the electromigration force is sufficiently strong that it overpowers the preference of the chain oxygen ions to order and begins to promote the displacement of all of the O(1) ions. The movement may proceed by the mechanism proposed by Rothman *et al.*[27] A calculation of the electromigration forces on chain oxygen ions with different nearest-neighbor configurations would be very helpful in quantifying this interpretation of our results.

The existence of the electromigration threshold allows us to employ the semiclassical theory of electromigration to estimate the atomic force necessary to overcome the favorable thermodynamical tendency of the basal-plane oxygen ions to order in YBCO. If we assume that the electron-wind contribution dominates, the electromigration force on the oxygen ions is

$$F_w \approx 2mv_F J_{\mathrm{EM}} \sigma / e \ , \tag{4}$$

where σ is the oxygen ion scattering cross section, m is the mass of the YBCO charge carrier, and v_F is the Fermi velocity. Assuming simply for the purpose of obtaining a numerical estimate that $\sigma \sim 10^{-15}$ cm^2, $v_F \approx 2.2 \times 10^7$ cm/s,[35] and using the free-electron value for m, we find $F_w \sim 10^{-9}$ dyn. While this number is at best only a rough estimate, it does indicate that a very low driving force can rapidly disorder the basal-plane oxygen in slightly oxygen-deficient YBCO.

The tendency of a microbridge to develop two distinct and fairly sharp resistive transitions (i.e., to exhibit a foot) following the application of a strong electromigration bias is indicative both of the ability of rather weak atomic forces to create chain site disorder in YBCO and of the tendency of this disorder to subsequently segregate or localize under the imposition of such a force. This suggests first that the chain oxygen mobility may be sufficient to permit longer-range motion than the 0.97-eV activation energy would otherwise indicate, and also demonstrates that the activation energy for the chain oxygen diffusion is very much a function of the local environment. This conclusion is emphasized by the ability to very significantly and reversibly change the T_c of the foot transition by electromigration without substantially affecting the "bulk" transition, as illustrated in Fig. 13.

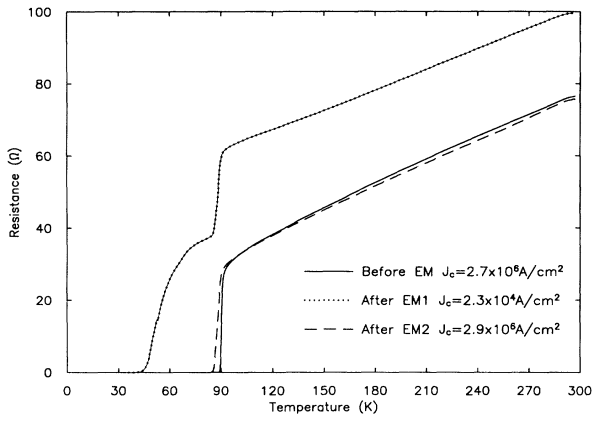

FIG. 13. Electromigration-induced damage and its reversal is illustrated again here. The reduction in J_c by 2 orders of magnitude is fully recovered by the subsequent current bias. EM(1) was done at a bias of 4.2 MA/cm^2 for 4 min and the subsequent electromigration EM(2) was performed with a bias of 3.5 MA/cm^2 in the opposite direction for 12 h. Note that the initial microbridge had a J_c about an order of magnitude lower than the best; this illustrates that regions that are not optimally ordered are relatively easily affected.

Once areas of high defect density (regions with a low T_c) are created, they are easily affected by lower currents, while regions of lower defect density ("good" regions with a high T_c) remain relatively unaffected.

To summarize, these electromigration experiments on grain-aligned YBCO films have demonstrated that the weak atomic forces that arise from a bias current density of ~ 5 MA/cm^2 are sufficient to quickly disorder the basal-plane oxygen at 350 K. This suggests that a rather small elastic strain gradient in a YBCO film, such as that found in the vicinity of a coherent grain boundary, could also be sufficient to locally suppress the superconductive state as a consequence of this disordering process, thus accounting for the very high sensitivity of the transport properties of YBCO to the presence of structural defects. To further examine this point we now turn to a discussion of electromigration effects in microbridges containing high-angle tilt boundaries.

IV. MICROBRIDGES CONTAINING HIGH-ANGLE TILT BOUNDARIES

A. On the character of high-angle tilt boundaries

The highly deleterious effects of high-angle tilt boundaries on the superconductive transport properties of the cuprate superconductors were clearly established very shortly after the discovery of high-T_c superconductivity. The pioneering work of Chaudhari *et al.*[36] that examined the critical current, I-V characteristic, and magnetic field dependence of small cross-sectional area tilt boundaries formed by epitaxial growth on $SrTiO_3$ bicrystals was the first attempt to quantify this grain-boundary effect. We have studied the structural[37–39] and transport[11,17,40] properties of isolated, high-angle tilt boundaries in YBCO microbridges in considerable detail, and we now give a summary of the relevant results.

The strong attenuation of the bulk or intracrystal J_c that is observed for transport across a tilt boundary has been attributed to the formation of a normal, or insulating, barrier at the boundary.[41,42] While impurity phases in poor high-T_c material can certainly result in such effects, examination of the grain boundaries in good thin films generally does not support this interpretation. High-resolution scanning transmission electron microscopy (STEM) and conventional transmission electron microscopy (TEM) have revealed no boundary layer or segregation of secondary phase within a few nm of the tilt boundary.[37–39] And energy dispersive X-ray (EDX) studies with a 2-nm spatial resolution indicate no local change in stoichiometry (including oxygen content to a level of 3 parts per 70) across the boundary.[37–39] In this latter case, some recent microscopy studies have focused on attributing the grain-boundary effect to the consequence of the dislocation network at the boundary in locally suppressing the superconductivity by elastic strain.[43]

The electrical evidence for the existence of a "Josephson grain-boundary junction" in thin-film microbridges containing a tilt boundary is generally taken from the temperature dependence of the intergrain I_c, from the I-

V characteristic, including the effects of thermal noise rounding[17,44] and rf radiation,[17] and, for samples which are narrower than the effective (Josephson) penetration depth, from the magnetic field dependence of I_c, all of which generally exhibit behavior that is reminiscent of that expected from a resistively shunted Josephson junction. However, the evidence is not conclusive, as we now discuss.

The intergrain J_c temperature dependence is generally very similar to that measured for the intragrain J_c, except perhaps near T_c, where the effects of a small spread in T_c for the material along the grain boundary can readily produce a T dependence for I_c that could otherwise be interpreted as indicating the presence of a normal layer.[17] The usual observation of a foot in the resistive transition of such a microbridge, which is correlated with the presence of the grain boundary, can be attributed to a normal-metal proximity effect locally suppressing T_c. This is illustrated in Fig. 14 for one of our tilt-boundary weak links. As we have shown above, however, such a foot can equally well be caused by a local suppression of T_c by chain oxygen disorder. Moreover, examination of tilt boundary I-V characteristics generally show some significant departure from the detailed prediction of the RSJ model, as do careful measurements of the ac Josephson response (Shapiro steps) to microwave radiation.[17]

Measurements of the dependence of the Shapiro step amplitude on rf power for tilt boundary weak links that exhibit RSJ-like I-V's with no discernible excess current have found significant quantitative deviations from the driven RSJ model.[17] The behavior is quite similar to that found much earlier[45,46] in the rf response of low-T_c thin-film two-dimensional mirobridges where the length of the microbridge was of the order of the superconductive coherence length ξ. The two-dimensional nature and finite length of those microbridge structures contributed to the fact that the suppression of the superconductive state by the very high bias current density was not sufficiently localized to yield a weak-link effect with ideal Josephson-like behavior,[47] unlike the behavior which is regularly found when a tunnel barrier or proximity effect from a normal-metal-layer provides the weak-link effect.

While I_c, for low-J_c boundaries, generally varies quasiperiodically with H, *close* agreement of $I_c(H)$ with the Josephson prediction has yet to be reported for a grain-boundary weak link. Further analysis of the magnetic field behavior of I_c generally indicates a strong nonuniformity in J_c across the breadth of the boundary, with the maximum variation in J_c being at least a factor of 10.[17] Since the *average* J_c in these high-angle (27° and 45°) boundaries is typically $\geq 5\times 10^4$ A/cm^2 at 4.2 K, this implies that the maximum J_c is much higher. As a particularly strong example of this effect, in Fig. 15 we show the RSJ-like I-V characteristic of a $\sim$1-μm-wide tilt-boundary weak link taken with zero H and with $H=3$ T. For low applied fields ($H\sim 0.01$ T), the critical current varies quasiperiodically with H, but persists with a significant value up to very high H. If we assume a typical value for the penetration depth of $\lambda\approx 0.2$ μm, this implies that the scale ζ of the lateral inhomogeneities in J_c of this tilt boundary is $\zeta\leq 10$ nm.

Finally, examination of recent measurements[48–50] of the $1/f$ noise of YBCO tilt-boundary weak links reveals that there are two, apparently independent, contributions to this noise. One noise component arises from the fluctuations δR of the weak-link resistance, the other from critical current fluctuations δI_c. A compilation of results from a number of devices indicate that these components do not scale with the cross-sectional area of the device, as is the case for tunnel junctions,[51] but rather that $\delta R/R\sim R^{0.5}$ and $\delta I_c/I_c\sim I_c^{-0.75}$. The resistance noise result is as expected if the $1/f$ noise arises from independent fluctuations of a parallel array of normal conductive connections and if changes in grain-boundary resistance arise simply from changes in the number of these parallel connections. The general dependence of the critical current $1/f$ noise on I_c is consistent with the noise arising from independent fluctuations of the critical currents

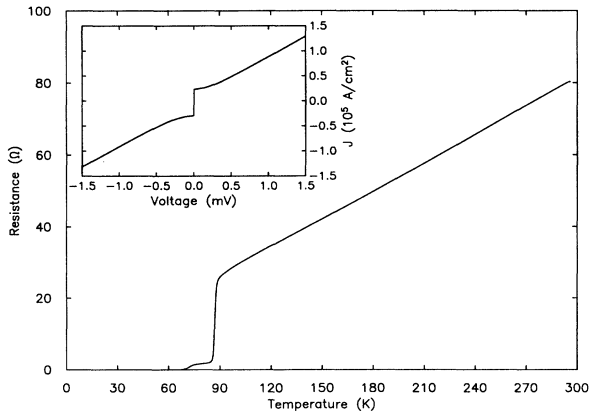

FIG. 14. The transition and I-V characteristic for a tilt-boundary weak link. The foot in the transition is characteristic of all well-behaved YBCO weak links, i.e., those displaying nearly ideal RSJ behavior, as seen in the I-V curve.

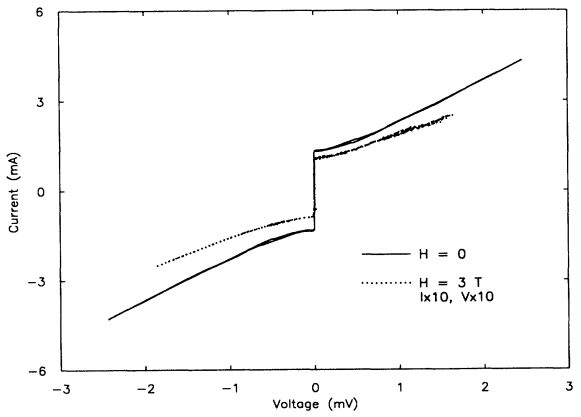

FIG. 15. The critical current of this weak link at the high field of 3 T was found to still be oscillating with small changes in the magnetic field. The local maximum shown here exhibited a critical current which was 7% of the zero-field value. This implies that the scale of lateral inhomogeneities along the grain boundary is on the order of 10 nm or less.

of a parallel array of superconductive connections. The somewhat stronger than $I_c^{-0.5}$ variation of the scaled noise indicates, however, that the number of fluctuators responsible for the critical current noise grows less rapidly than does the area of superconductive connections when the critical current density of grain boundaries increases.

Thus, the picture that emerges from this brief review is that high-angle tilt boundaries are bridged by an array of superconductive connections and by another array of normal paths that do not carry supercurrent. The fact that the amplitude of the scaled resistance fluctuations $\delta R/R$ is typically much less than $\delta I_c/I_c$ indicates that the number of superconductive connections is very significantly less than the number of normal connections, a result that is consistent with the much lower than expected I_cR_n value of grain-boundary weak links and that is also roughly consistent with the general scaling behavior of I_cR_n with weak-link conductance.[11] As we discuss below, the results of electromigration experiments on microbridges containing tilt-boundary weak links are in accord with this picture.

B. Electromigration results

The properties of microbridges containing high-angle tilt boundaries are substantially altered by considerably lower electromigration current densities (~ 2 MA/cm^2) than is the case for grain-aligned microbridges. Current densities at this level readily raise R_n, lower J_c, and create large feet in the transitions. Again there is a threshold, which varies from sample to sample, for the disordering effect where only somewhat lower values of J_{EM} will slowly improve the normal-state resistance and weak-link properties rather than degrade them. A typical example of degradation is shown in Fig. 16 where, as result of a bias of 2.5 MA/cm^2 for 130 min, R_n is more than doubled, T_c is decreased substantially, and J_c is decreased by about a factor of 10. Note also that the shape of the I-V characteristic has substantially changed. What began as a good, RSJ-like I-V has changed to something with a more rounded onset as might be observed in a long ($l \gg \xi_{ab}$) thin wire with some variation in I_c along its length.[52,53] This indicates that the effect of the electromigration current is to increase the disorder over a comparably long ($\gg \xi_{ab}$) distance from the grain boundary, rather than just to locally increase the grain-boundary weak-link effect.

As in the case of grain-aligned microbridges, the effects of electromigration can be reversed to some degree by applying an electromigration current in the opposite direction. Figure 17 illustrates this process for the weak link in Fig. 16. J_c is raised to its original value, R_n is decreased, and T_c is raised. The original shape of the I-V characteristic is not fully recovered, however. This indicates a general healing process throughout the degraded region, like that seen previously, and not a relocalization of defects back to the grain boundary.

In Fig. 18 is shown the results of electromigration on a microbridge that apparently contained two high-angle tilt boundaries, resulting in two weak links in series with

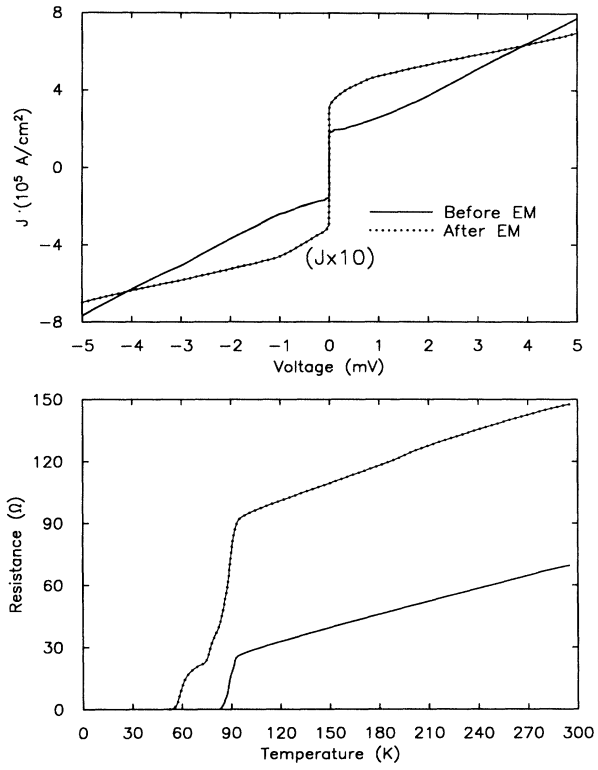

FIG. 16. Microbridges containing high-angle tilt boundaries are easily affected by the application of a current bias, as illustrated here. A bias of 2.5 MA/cm^2 for 2 h results in a large decrease in J_c (a) and a significant change in the character of the I-V curve. The resistive transition, R_n, and T_c are also severely affected (b).

somewhat different I_c's, which are clearly discernible in the I-V. Electromigration in this case increased the I_c and decreased R_n of one weak link, while it decreased the I_c and increased R_n of the other. These two tilt-boundary weak links appear to be due to a single misaligned grain in the microbridge which is bordered on both sides by grains that are in epitaxial alignment with the substrate. The electromigration behavior can then be understood in terms of the migration of disorder away from one tilt boundary and towards the other if the oxygen disorder is greater in the central, misaligned grain than in the adjoining, aligned grains. This does not imply that oxygen defects are rapidly moving a distance of ~ 1 μm under the electromigration force, but simply that some of the disorder in the central grain that was originally adjacent to the one boundary is being reduced, while the disorder is being increased at the other. This is further evidence for the idea that misoriented grains grow with more oxygen defects incorporated into them than do aligned grains. This idea is supported by earlier work on polycrystalline films.[16,54] The higher defect density may well be due to an increased lattice mismatch strain of rotated grains. It would be very useful to study the strain difference between films aligned with the underlying substrate and films grown fully rotated. Indeed,

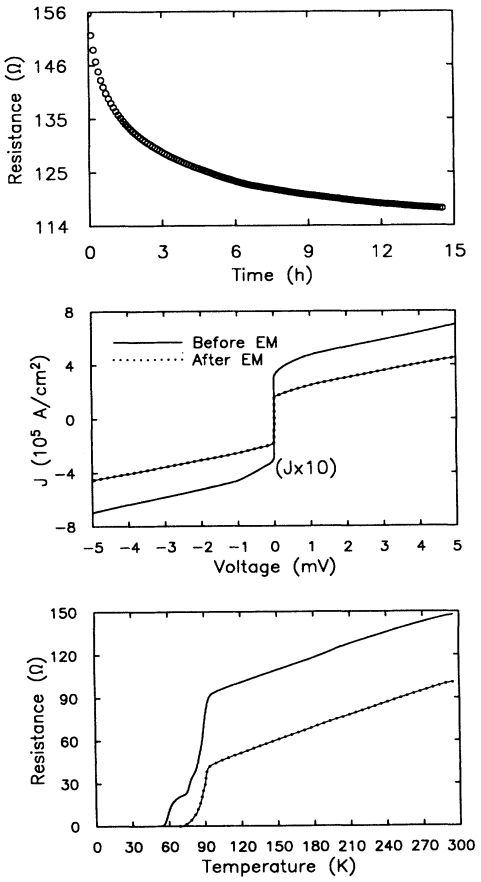

FIG. 17. Reversal of the damage done to the weak-link microbridge in Fig. 16. The bias level in this case was 2 MA/cm^2 in a direction opposite to the previous bias. The resistance vs time during this electromigration again follows the usual functional form of Eq. (1). Note that the RSJ-like shape of the original I-V curve (Fig. 16) is not recoverable.

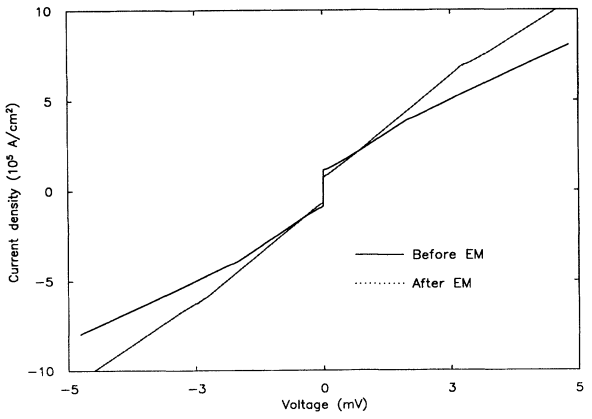

FIG. 18. This microbridge contains two weak links in series, attributable to the presence of two high-angle tilt boundaries. Electromigration at 2 MA/cm^2 for 12 h increased the I_c of one weak link and decreased the I_c of the other. The resistance of the two weak links also changed, in the opposite manner to the change in critical current.

Chew *et al.*[55] have seen significantly broadened x-ray peaks for films which are uniformly rotated about the *c* axis with respect to MgO. This again indicates a degradation in crystalline quality for rotated films. And there is already evidence that a reduction in thermal mismatch stress incorporated in the films forming biepitaxial grain-boundary weak links improves their superconductive properties.[56]

The time dependence for the current-driven healing of the resistance of microbridges that contain tilt boundaries is generally fit by the same type of stretched exponential function as is found for the grain-aligned microbridges [Eq. (1)]. Above the threshold for degradation, the rate of resistance change for these tilt-boundary microbridges is generally sufficiently slow that the time dependence of the process can be examined. As illustrated in Fig. 19, the functional form is very similar to the healing behavior except that now the resistance is increasing with a stretched-exponential time dependence rather than decreasing.

We interpret the slower rate of increase of R above threshold as indicating that the change is occurring only locally, in the vicinity near the tilt boundaries, rather than more globally throughout the microbridge, as appears to be the case for the microbridges without tilt boundaries. The lower threshold indicates that we begin with a greater degree of disorder, such as a high vacancy

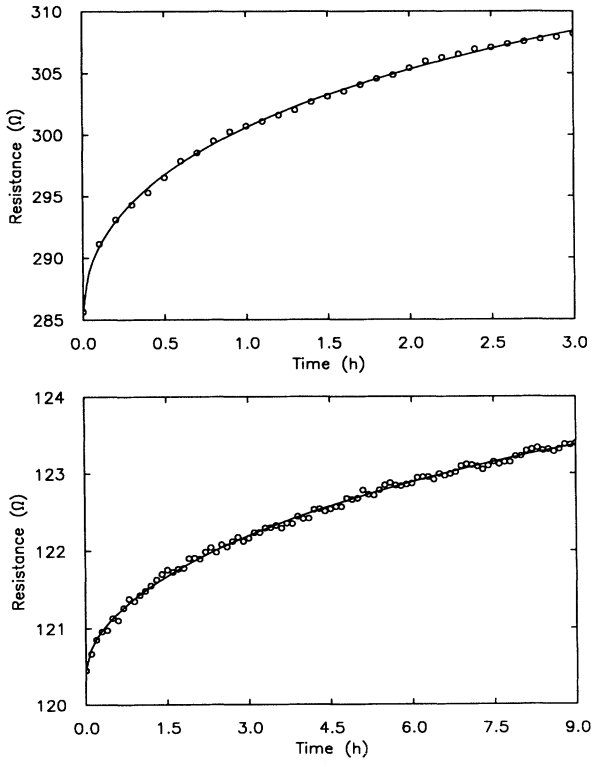

FIG. 19. The resistance vs time during electromigration of two microbridges containing high-angle tilt boundaries in which the properties were degraded. The lines are fits to the stretched-exponential functional form [Eq. (1)]. The bias current in the top plot was 2 MA/cm^2; the level was 2.4 MA/cm^2 in the lower figure.

density, near the boundaries since, as discussed above, the electromigration measurements on microbridges without tilt boundaries have shown that regions which had been significantly degraded by high currents can be subsequently affected by considerably lower currents. This further suggests that the cause for a foot in the resistive transition of microbridges with tilt boundaries is due to strong oxygen disorder. The time dependence of the degradation indicates again that there is a distribution of activation energies for the oxygen displacement. Taken together with the lower threshold near the tilt boundaries we conclude that the more disordered a region, the lower is the force required for the oxygen displacement that will increase that disorder.

V. DISCUSSION

In this section we will compare the key results of these electromigration studies of the effect of oxygen disorder in YBCO thin-film microbridges with and without high-angle tilt boundaries. From this comparison and with the benefit of earlier observations of the electrical properties of YBCO tilt-boundary weak links we will attempt to develop an improved picture of how such boundaries profoundly affect the normal-state and superconductive properties of this material.

A. Comparison of grain-aligned and tilt-boundary microbridge results

The behavior of the grain-aligned microbridges containing local concentrations of high oxygen disorder caused by electromigration has both similarities and important differences with the behavior of microbridges containing tilt-boundary weak links, either before or after they have undergone electromigration. Both types of microbridges regularly show resistive transitions consisting of one transition near the bulk value of T_c, which is due to the transition of the majority of microbridge material, and a lower transition (the foot) which is attributed to the suppressed transition of a disordered region or regions. Typically the sample resistance is approximately T independent between the main transition and the foot; this result is consistent with the fact that tilt-boundary weak links generally exhibit a T-independent normal-state resistance when biased well above their critical current. For both types of microbridges we generally find that the larger the resistance of the foot, the smaller the value of J_c and the greater the suppression of T_c; we also find that the greater the suppression of T_c, the greater is the reduction in J_c. These are correlations, however, not strict relations, and considerable variation is found from sample to sample. The minimum critical currents of both types of microbridges also have similar dependences on magnetic field for high values of H.

The most notable difference between the behavior of the two types of microbridges is that for a given suppression of T_c the critical current of a tilt boundary weak link is typically an order of magnitude or more lower than that of the disordered region of a grain-aligned microbridge. Figure 12 showed J_c, measured at 4.2 K, plotted vs T_c as determined by the zero resistance point of a grain-aligned microbridge following a series of electromigrations. Also shown in that figure are values of J_c (at 4.2 K) and T_c for a number of microbridges on MgO containing 45° and 27° high-angle tilt boundaries. Clearly the effect of the tilt boundary on J_c is due to more than the suppression of the transition temperature due to local oxygen disorder; the tilt boundary J_c is much lower, and, although there is considerable spread in the data, there is some indication that J_c decreases more rapidly with T_c for the tilt-boundary case.

We have argued that a strongly disordered grain-aligned microbridge has the characteristics of a composite consisting of a network of superconductive filaments where short breaks in the filaments can be bridged by normal-conductive paths contributing an essentially T-independent conductivity. As the oxygen disorder grows, the volume fraction of the superconductive component decreases, and the conductivity of the bridging connections begins to dominate. At a still higher degree of average oxygen chain disorder the material is effectively insulating although small superconductive inclusions may remain. The I-V characteristics of strongly disordered grain-aligned microbridges generally indicate that the average density of superconductive connections is "uniform" over a characteristic length scale $d \gg \xi_{ab}$, or that the microbridge consists of a series of weak links. In contrast, the fairly RSJ-like I-V characteristics of many tilt-boundary weak links indicate that the weak-link extent in the direction normal to the boundary is $\approx \xi_{ab}$.

B. A tilt-boundary model

These observations may be explained by a phenomenological model of how the presence of a tilt boundary can exacerbate the effect of disorder in the regions adjacent to the boundary. The initial effect of a grain boundary is to create an elastic strain gradient which, if it is sufficiently strong, can result (in the same way as a strong electromigration current) in the local disordering of the chain oxygen and in the segregation of defects to the vicinity of the boundary. If the effect is sufficient to substantially depress T_c, then we deduce from the measurements of J_c in disordered grain-aligned microbridges that the fraction of the composite material that is still superconductive in the cross section next to the grain boundary is much less than one. In the absence of detailed microscopic insight we assume that the existing superconductive filaments are randomly distributed throughout this cross section, with again the size scale of these filaments being anywhere in the range from ζ (60 nm) to ξ_{ab} ($\sim$1 nm). Assume that p is the probability that an element adjacent to the grain boundary is superconductive; this element has an area equal to the average area of the superconductive filaments. Then if the spatial distributions of filaments for the two adjoining grains are uncorrelated, the likelihood of a superconductive contact bridging the boundary is simply the square of the probability p. An "artist's conception" of a two-dimensional version of this idealized model is shown in Fig. 20. The nature of the superconductive contact between the filaments is not fixed in this

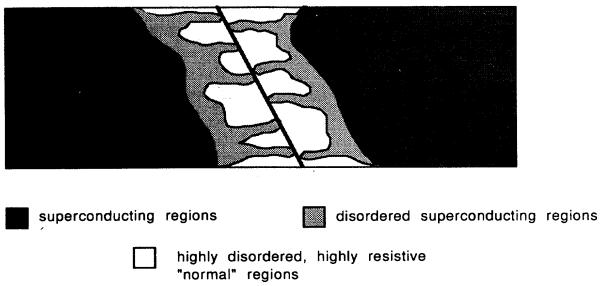

FIG. 20. A two-dimensional representation of the phenomenological model of a high-angle tilt-boundary weak link in YBCO. Filaments of superconducting material that are sufficiently disordered to suppress T_c but with otherwise bulk-like properties, are distributed on both sides of the grain boundary represented here by a solid line. When two such filaments abut each other, the result is a contact that supports a supercurrent. The highly disordered material provides normal resistance connections between filaments that do not closely align. The primary features of this model account for an array of experimental grain-boundary weak-link data.

model. The contact could either be a thin tunnel barrier, a very abrupt superconductor–normal-metal–superconductor (SNS) contact, or an *S-c-S* "nanobridge" constriction. As noted above, the rf Josephson data and nonideal *I-V* characteristics of most tilt-boundary weak links favor the latter possibility. Whatever the exact nature of the contact, we note that it appears to be, in fact, a rather strong weak link, with the reduction in J_c from that of the immediately adjoining material apparently being only a factor of order 0.1, indicating that the tunnel barrier, if it exists, is quite thin indeed compared to conventional tunnel barriers where a very thin barrier results in a reduction of J_c of $\sim 10^{-3}$.

The supposition that the distribution of superconductive filaments is uncorrelated from grain to grain is quite reasonable for the case of high-angle boundaries, particularly if the dominant pathway for oxygen diffusion that creates these filaments is along the *b* axis. A high-angle boundary could act to break this diffusion pathway, as well as provide a via for oxygen loss from the film by diffusion along the boundary. Thus, for example, if two adjoining grains each have a suppressed T_c of 80 K for the material adjacent to the boundary, i.e., within a few coherence lengths, the low-temperature measurement of J_c for electromigrated microbridges suggests that only 10% of this material is effectively superconductive. This observation, in the context of our proposed model, suggests that the grain boundary J_c at low T should be of the order of 1% of that of well-ordered single-crystal material with strong pinning. This is roughly consistent with our tilt-boundary results.

Of course, the distribution of superconductive elements or filaments in the material along two sides of the grain boundary may not be random, due to particular details of the growth process, extended defects in the epitaxial substrate, and/or nonuniform strain along each side of the tilt boundary. Then the effect of the boundary in breaking superconductive connections will differ in magnitude from the case of a random distribution. If the average superconductive areal density of the adjacent material is much less than one, the result would be a stronger suppression in J_c for a given suppression in T_c. Such lower values of J_c have sometimes been found in studies of tilt boundaries formed by thin-film biepitaxial approaches.[56]

C. Scaling behavior and the effect of tilt-boundary angle

Some time ago Russek *et al.*[11] reported the observation of a scaling behavior for the I_cR_n value of tilt-boundary weak links. For several weak links it was found that I_cR_n varied rather closely as $J_c^{1/2}$, or equivalently as σ_n, where σ_n is the conductance per unit area of the weak link. This scaling also described changes in I_c and R_n that would occur upon partial oxygen removal by rapid annealing at 500 °C in argon. A similar, but somewhat different, scaling behavior was subsequently reported by Gross *et al.*[57] for weak links created by thin-film growth on $SrTiO_3$ bicrystals. Recent measurements by Char *et al.*[56] on 45° tilt boundaries formed by their biepitaxy process have also demonstrated a scaling behavior, but one that varied depending on the details of the particular biepitaxial process employed. Figure 21 summarizes much of the available data on this phenomenon. There is clearly considerable variation from one class of tilt boundaries to another, but the general trend for I_cR_n to increase with J_c (or with σ_n) is quite evident.

All values of R_n that have been reported for well-characterized tilt-boundary weak links are quite a bit lower than the ideal value that would be expected from an ideal tunnel barrier, a small ideal superconductive contact, or a thin normal-metal SNS contact. Thus, this resistance can be presumed to arise from the nonideal ohmic shunting of the superconductive connection. We have seen that moderate oxygen disorder in YBCO films results in what has the character of a normal resistive shunt in parallel with a network of superconductive filaments. Therefore, a superconductive filament on one side of a tilt boundary which does not align with another such filament on the other side is likely to result in an ohmic shunting of the ideal resistance that would be displayed by these bridging connections when driven normal. The conductance σ_n of the tilt boundary should then scale with p, and thus we would have $I_cR_n \propto \sigma_n$, in agreement with the original observations on 45° tilt boundaries formed on single-crystal MgO.

Of course, not all tilt boundaries are necessarily bounded by the same degree of oxygen disorder in each of the two adjacent grains, and, as noted above, in each case this disorder may well not be randomly distributed along the width of the boundary. This will depend on the details of the growth process that creates these tilt boundaries. As we have already discussed, for the case of films grown with two different orientations of the grains on a single-crystal substrate, such as the MgO case being studied here, there is significant evidence that the orientation of a YBCO grain with respect to the substrate is a

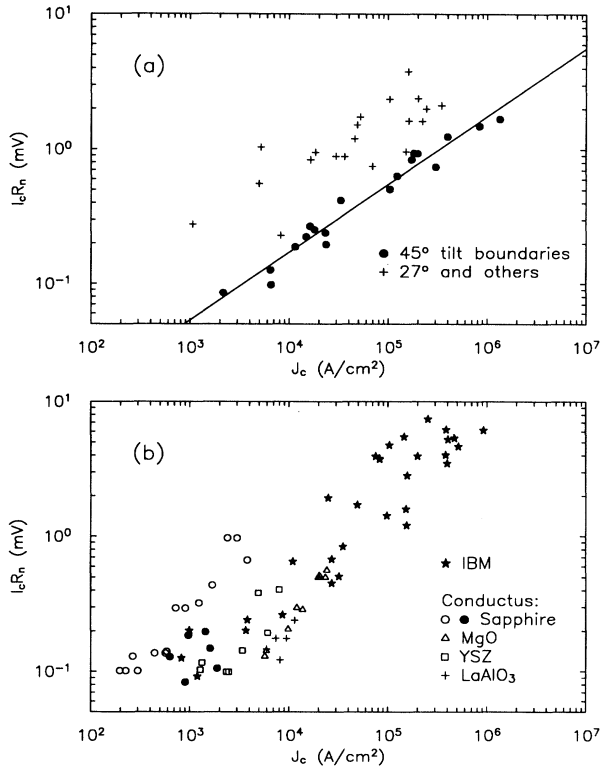

FIG. 21. The scaling behavior of the I_cR_n products for several types of tilt-boundary weak links. The quantity J_c is the average critical current density of the weak link. Data from several of our weak links are shown in (a). The line is the best fit to the data from our 45° tilt-boundary microbridges; the slope is 0.505. This indicates that $I_cR_n \propto J_c^{1/2}$, or equivalently, $I_cR_n \propto \sigma_n$, where σ_n is the conductance per unit area. The lower figure (b) plots data from IBM's bicrystal weak links (Ref. 57) and from Conductus's biepitaxial weak links using the various substrate materials listed (Ref. 56).

major factor in determining the degree of oxygen order in the grain. In addition to grain-aligned and 45° tilt-boundary microbridges, we have previously studied the properties of microbridges which contain 27° tilt boundaries.[58] We find that the most favorable orientation is with the principal axes of the YBCO grain and MgO (001) substrate being in close alignment, the next most favorable orientation is the 45° rotation of the YBCO grain about the c axis, with the 27° misalignment being the least favorable. As a result, in this situation we find that 45° tilt boundaries formed between aligned and rotated grains on MgO substrates generally have considerably higher J_c's and higher conductance than do 27° tilt boundaries formed in a similar manner. In addition, simulations of the spatial variation of the critical current across the microbridge obtained from magnetic field measurements have shown that 27° tilt boundaries have a much more highly nonuniform J_c than do 45° boundaries.[58] These results are contrary to the results obtained with high-angle tilt boundaries formed by growth on bicrystal substrates.[41]

In the context of the proposed phenomenological model of a tilt boundary, if one of the two adjoining grains has a different degree of oxygen disorder adjacent to the boundary than does the other, then J_c will vary as p_1p_2, where p_i is the probability that a given element on one of the two sides of the boundary is sufficiently ordered to be superconductive. On the other hand, the shunt conductance should then vary as (p_1+p_2). If $p_1 \gg p_2$ we have $I_cR_n \propto p_2$, i.e., is largely independent of σ_n. This can account for the fact that I_cR_n for 27° tilt boundaries follows a somewhat different scaling behavior (see Fig. 21), varying less rapidly with J_c, or σ_n, than do many of the 45° boundaries which appear to be bounded on both sides by material that is somewhat more equally ordered.

The variation in the data of Fig. 21 of tilt-boundary weak links formed by methods other than natural grain growth may also be explained by appeal to the idea of nonsymmetric order on each side of the tilt boundary. In the case of tilt boundaries formed by growth on bicrystal and biepitaxial substrates there is likely to be a tendency for these boundaries to be locally bounded by unequal degrees of oxygen disorder. It is known that YBCO thin films tend to form by island nucleation and growth.[59] Thus, the grain boundary in the bicrystal film does not necessarily exactly coincide with the substrate boundary, since a grain in the film may grow past this boundary before encountering another thin-film grain of the other orientation. Given the very short coherence length, only a few nm's displacement can suffice to materially degrade the oxygen order in that portion of the grain that is now misaligned with the substrate to the point where the superconductive properties are locally suppressed much more than for the opposing grain. In the biepitaxial approach the two YBCO films are formed on different thin-film templates and thus a global asymmetry in the disorder may well be expected, in addition to the local asymmetry generated by grain overgrowth. These ideas are supported by some of the observations made in recent TEM analysis of these biepitaxial weak links.[60] We note that Char *et al.*[56] were able to very substantially improve their critical current densities by adapting a different substrate material system that had a reduced thermal expansion mismatch.

VI. SUMMARY AND CONCLUSIONS

The results of this study have again highlighted the central role of oxygen in determining the normal-state and superconductive properties of YBCO. In this paper we have described the remarkable effects of large current biases on YBCO thin-film microbridges. We attribute these effects to the electromigration of oxygen defects. Below a certain threshold, the properties of YBCO are improved due to a reordering of these defects in the basal plane. For current biases above the threshold, these properties are degraded. The time dependence for the effects of electromigration are characteristic of a system with a distribution of activation energies. This suggests that the dispersive transport of defects is involved and indicates a variation in the effective binding energy of the chain oxygen with the local environment. The compelling difference in behavior above and below threshold al-

lows us to obtain an estimate for the force needed to overcome the tendency for the oxygen to order. The relatively low value of this force elucidates one of the primary problems with the high-T_c materials. In addition to these observations, it was discovered that the effects caused by electromigration are reversible, pointing out the ease by which the oxygen defects can segregate to the myriad structural defects in the material.

We have observed that the superconductive properties of the disordered regions caused by electromigration are indicative of a filamentary superconductive system shunted by nonsuperconductive ohmic paths. Thus, the locally nonuniform nature of disordered YBCO is apparent, as are the resulting dramatic effects on the superconductive properties.

The results of this study have enabled us to draw general parallels between the bulk thin-film behavior and the effects due to grain boundaries. It is seen that the tilt boundaries can be viewed as areas of superconductive connections of the already-present filaments. Our phenomenological model is consistent with a wide array of experimental results, including I_cR_n scaling behavior, $1/f$ noise data, magnetic field effects, rf response, and other transport measurements, as well as oxygenation studies and electron microscopy analysis.

ACKNOWLEDGMENTS

We wish to acknowledge the many contributions provided to this work by D. H. Shin, J. Silcox, Jian Li, James Mayer, and Grant Norton. This research was supported by the Office of Naval Research, Contract No. N00014-89-J-1692, and, in part, by the Defense Advanced Research Projects Agency through the Consortium for Superconducting Electronics. Additional support was received from the National Science Foundation through use of the facilities of the National Nanofabrication Facility and the Cornell Materials Science Center. B.H.M. acknowledges support by the U.S. Department of Education.

[1]B. W. Veal, H. You, A. P. Paulikas, H. Shi, Y. Fang, and J. W. Downey, Phys. Rev. B **42**, 4770 (1990).
[2]B. W. Veal, A. P. Paulikas, H. You, H. Shi, Y. Fang, and J. W. Downey, Phys. Rev. B **42**, 6305 (1990).
[3]H. Claus, S. Yang, A. P. Paulikas, J. W. Downey, and B. W. Veal, Physica C **171**, 205 (1990).
[4]J. D. Jorgensen, S. Pei, P. Lightfoot, H. Shi, A. P. Paulikas, and B. W. Veal, Physica C **167**, 571 (1990).
[5]R. J. Cava, A. W. Hewat, E. A. Hewat, B. Batlogg, M. Marezio, K. M. Rabe, J. J. Krajewski, W. F. Peck, Jr., and L. W. Rupp, Jr., Physica C **165**, 419 (1990).
[6]G. Ceder, R. McCormack, and D. de Fontaine, Phys. Rev. B **44**, 2377 (1991).
[7]D. de Fontaine, G. Ceder, and M. Asta, Nature (London) **343**, 544 (1990).
[8]R. P. Gupta and M. Gupta, Phys. Rev. B **44**, 2739 (1991).
[9]H. F. Poulsen, N. H. Andersen, J. V. Andersen, H. Bohr, and O. G. Mouritsen, Nature (London) **349**, 594 (1991).
[10]B. W. Veal and A. P. Paulikas, Physica C **184**, 321 (1991).
[11]S. E. Russek, D. K. Lathrop, B. H. Moeckly, R. A. Buhrman, D. H. Shin, and J. Silcox, Appl. Phys. Lett. **57**, 1155 (1990).
[12]S. Vitta, M. A. Stan, J. D. Warner, and S. A. Alterovitz, Appl. Phys. Lett. **58**, 759 (1991).
[13]K. Rajan, P. Parameswaran, J. Janaki, and T. S. Radhakrishnan, J. Phys. D **23**, 694 (1990).
[14]D. Robbes, A. H. Miklich, J. J. Kingston, Ph. Lerch, F. C. Wellstood, and J. Clarke, Appl. Phys. Lett. **56**, 2240 (1990).
[15]L. F. Rybal'chenko, V. V. Fisun, N. L. Bobrov, I. K. Yanson, A. V. Bondarenko, and M. A. Obolenskii, Fiz. Nizk. Temp. **17**, 202 (1991) [Sov. J. Low Temp. Phys. **17**, 105 (1991)].
[16]B. H. Moeckly, S. E. Russek, D. K. Lathrop, R. A. Buhrman, J. Li, and J. W. Mayer, Appl. Phys. Lett. **57**, 1687 (1990).
[17]D. K. Lathrop, B. H. Moeckly, S. E. Russek, and R. A. Buhrman, Appl. Phys. Lett. **58**, 1095 (1991); see also IEEE Trans. Magn. **27**, 3203 (1991).
[18]S. J. Hagen, T. W. Jing, Z. Z. Wang, J. Horvath, and N. P. Ong, Phys. Rev. B **37**, 7928 (1988).
[19]T. A. Friedmann, J. P. Rice, J. Giapintzakis, and D. M. Ginsberg, Phys. Rev. B **39**, 4258 (1989).
[20]G. Weigang and K. Winzer, Z. Phys. B **77**, 11 (1989).
[21]B. Planpain, R. Revesz, L. R. Doolittle, K. H. Purser, and J. W. Mayer, Nucl. Instrum. Methods B **34**, 459 (1988).
[22]J. Li, B. H. Moeckly, and R. A. Buhrman (unpublished).
[23]G. Koren, A. Gupta, E. A. Giess, A. Segmuller, and R. A. Laibowitz, Appl. Phys. Lett. **54**, 1054 (1989).
[24]J. D. Jorgensen, D. G. Hinks, P. G. Radaelli, S. Pei, P. Lightfoot, B. Dabrowski, C. U. Segrè, and B. A. Hunter, Physica C **185-189**, 184 (1991).
[25]T. A. Friedmann, M. W. Rabin, J. Gianpintzakis, J. P. Rice, and D. M. Ginsberg, Phys. Rev. B **42**, 6217 (1990).
[26]S. J. Rothman, J. L. Routbort, and J. E. Baker, Phys. Rev. B **40**, 8852 (1989).
[27]S. J. Rothman, J. L. Routbort, U. Welp, and J. E. Baker, Phys. Rev. B **44**, 2326 (1991).
[28]M. Ronay and P. Nordlander, Physica C **153-155**, 834 (1988).
[29]F. Kohlrausch, Pogg. Ann. Phys. **119**, 352 (1863).
[30]G. Williams and D. C. Watts, Trans. Faraday Soc. **66**, 80 (1970).
[31]A. Plonka, *Time-Dependent Reactivity of Species in Condensed Matter*, Lecture Notes in Chemistry **40** (Springer-Verlag, New York, 1986).
[32]J. Klafter, M. F. Schlesinger, Proc. Natl. Acad. Sci. USA **83**, 848 (1986).
[33]H. F. Poulsen, N. H. Andersen, J. V. Andersen, H. Bohr, and O. B. Mouritsen, Phys. Rev. Lett. **66**, 465 (1991).
[34]J. Bardeen, Rev. Mod. Phys. **34**, 667 (1962).
[35]P. B. Allen, W. E. Pickett, H. Krakauer, Phys. Rev. B **37**, 7482 (1988).
[36]P. Chaudhari, J. Mannhart, D. Dimos, C. C. Tsuei, C. C. Chi, M. M. Oprysko, and M. Scheuermann, Phys. Rev. Lett. **60**, 1653 (1988).
[37]D. H. Shin, J. Silcox, S. E. Russek, D. K. Lathrop, B. H. Moeckly, and R. A. Buhrman, Appl. Phys. Lett. **57**, 508 (1990).
[38]D. H. Shin, J. Silcox, D. K. Lathrop, S. E. Russek, B. Moeckly, and R. A. Buhrman, in *Science and Technology of Thin Film Superconductors 2,* edited by R. D. McConnell and R. Noufi (Plenum, New York, 1990), p. 319.
[39]D. H. Shin, J. Silcox, S. E. Russek, D. K. Lathrop, and R. A. Buhrman, in *High-Temperature Superconductors: Fundamen-*

tal Properties and Novel Materials Processing, edited by D. Christen *et al.*, MRS Symposia Proceedings No. 169 (Materials Research Society, Pittsburgh, 1990), p. 773.

[40]B. H. Moeckly, D. K. Lathrop, G. F. Redinbo, S. E. Russek, and R. A. Buhrman, in *High-Temperature Superconductors: Fundamental Properties and Novel Materials Processing*, edited by D. Christen *et al.*, MRS Symposia Proceedings No. 169 (Materials Research Society, Pittsburgh, 1990), p. 1193.

[41]J. Mannhart, P. Chaudhari, D. Dimos, C. C. Tsuei, and T. R. McGuire, Phys. Rev. Lett. **61**, 2476 (1988).

[42]D. Dimos, P. Chaudhari, and J. Mannhart, Phys. Rev. B **41**, 4038 (1990).

[43]M. F. Chisholm and S. J. Pennycook, Nature (London) **351**, 47 (1991).

[44]R. Gross, P. Chaudhari, D. Dimos, A. Gupta, and G. Koren, Phys. Rev. Lett. **64**, 228 (1990).

[45]W. Henkels, Ph.D. thesis, Cornell University, 1974.

[46]M. Octavio, W. J. Skocpol, and M. Tinkham, Phys. Rev. B **17**, 159 (1978); M. Tinkham, M. Octavio, and W. J. Skocpol, J. Appl. Phys. **48**, 4054 (1974).

[47]L. D. Jackel, W. H. Henkels, J. M. Warlaumont, and R. A. Buhrman, Appl. Phys. Lett. **29**, 214 (1976).

[48]L. Pesenson, B. H. Moeckly, and R. A. Buhrman (unpublished).

[49]M. Kawasaki, P. Chaudhari, and A. Gupta, Phys. Rev. Lett. **68**, 1065 (1992).

[50]A. H. Miklich, J. Clarke, M. S. Colclough, and K. Char, Appl. Phys. Lett. **60**, 1899 (1992).

[51]C. T. Rogers and R. A. Buhrman, IEEE Trans. Magn. **MAG-21**, 126 (1985); Phys. Rev. Lett. **53**, 1272 (1984).

[52]W. J. Skocpol, M. R. Beasley, and M. Tinkham, J. Appl. Phys. **45**, 4054 (1974).

[53]M. Tinkham, Adv. Solid State Phys. 363 (1979).

[54]B. H. Moeckly, S. E. Russek, D. K. Lathrop, R. A. Buhrman, M. G. Norton, and C. B. Carter, Appl. Phys. Lett. **57**, 2951 (1990); see also IEEE Trans. Magn. **27**, 1017 (1991).

[55]N. G. Chew, S. W. Goodyear, R. G. Humphreys, J. S. Satchell, J. A. Edwards, and M. N. Keene, Appl. Phys. Lett. **60**, 1516 (1992).

[56]K. Char, M. S. Colclough, L. P. Lee, and G. Zaharchuk, Appl. Phys. Lett. **59**, 2177 (1991).

[57]R. Gross, P. Chaudhari, M. Kawasaki, and A. Gupta, Phys. Rev. B **42**, 10 735 (1990).

[58]D. K. Lathrop, Ph.D. thesis, Cornell University, 1991.

[59]M. G. Norton, C. B. Carter, B. H. Moeckly, S. E. Russek, and R. A. Buhrman, in *Science and Technology of Thin Film Superconductors 2*, edited by R. D. McConnell and R. Noufi (Plenum, New York, 1990), pp. 379–387.

[60]S. J. Rosner, K. Char, and G. Zaharchuk, Appl. Phys. Lett. **60**, 1010 (1992).